Sigma Journal of Engineering and Natural Sciences
Web page info: https://sigma.yildiz.edu.tr
DOI: 10.14744/sigma.2026.1990

Research Article

Development of plant extract-loaded electrospun nanofiber for the prevention of biofilm-associated infections

Sevim Feyza ERDOĞMUŞ[1,*], Cengiz SARIKURKCU[2]

[1]*Department of Pharmaceutical Microbiology, Faculty of Pharmacy, Afyonkarahisar Health Sciences University, Afyonkarahisar, 03030, Türkiye*
[2]*Department of Analytical Chemistry, Faculty of Pharmacy, Afyonkarahisar Health Sciences University, Afyonkarahisar, 03030, Türkiye*

ARTICLE INFO

Article history
Received: 23 August 2024
Revised: 14 October 2024
Accepted: 05 February 2025

Keywords:
Astragalus Lusitanicus; Biological Activity; Chemical Composition; Electrospinning; Nanofiber

ABSTRACT

Antibiotic resistance has emerged as a critical global health challenge, complicating the treatment of infectious diseases. The bioactive compounds present in plants offer promising avenues for addressing antibiotic resistance, particularly when combined with advanced biotechnological approaches. This study aimed to develop plant extract-loaded electrospun nanofibers for preventing biofilm-associated infections, with a focus on the antimicrobial and antibiofilm properties of *Astragalus lusitanicus* subsp. *orientalis*. Phytochemical analysis of the plant extract was conducted using liquid chromatography-electrospray tandem mass spectrometry, identifying hesperidin (7864 µg/g) as the most abundant compound, followed by quercetin (2223 µg/g) and hyperoside (1804 µg/g). Electrospun nanofibers were successfully fabricated, incorporating the plant extract, and characterized using scanning electron microscopy, and Fourier-transform infrared spectroscopy. *In vitro* tests revealed the nanofibers' favorable properties, including uniform morphology, flexibility, and ease of handling. Antimicrobial activity was evaluated via disc diffusion and broth microdilution assays, demonstrating significant effects against *Klebsiella pneumoniae* (24±1.25 mm zone of inhibition) and other pathogens at varying concentrations. Notably, *Staphylococcus aureus* ATCC 25923 and *Bacillus subtilis* NRS 744 were resistant. Antibiofilm assays showed that plant extract-loaded nanofibers and the plant extract inhibited biofilm formation by 96% and 82%, respectively, against biofilm-producing *Staphylococcus aureus* ATCC 25923, as confirmed by SEM. This study highlights the potential of *Astragalus lusitanicus* subsp. *orientalis* as a source of antimicrobial agents and demonstrates the synergistic benefits of integrating its extract into nanofibers. The findings provide a foundation for industrial applications in antimicrobial therapies and tissue engineering, emphasizing the high biocompatibility and controlled release properties of the nanofiber system. For the first time, the antibiofilm effects of this plant species are reported, underscoring its potential in accelerating the healing process and combating biofilm-associated infections.

Cite this article as: Erdoğmuş SF, Sarıkurkcu C. Development of plant extract-loaded electrospun nanofiber for the prevention of biofilm-associated infections. Sigma J Eng Nat Sci 2026;44(1):423–438.

***Corresponding author.**
*E-mail address: feyza.erdogmus@afsu.edu.tr

This paper was recommended for publication in revised form by Editor-in-Chief Ahmet Selim Dalkilic

INTRODUCTION

Antibiotics are typically employed in the treatment of infectious diseases. However, the emergence of antibiotic resistance has emerged as a significant global concern. Therefore, the treatment of infectious diseases by these microorganisms has become difficult. In addition, some microorganisms produce biofilm and researchers have determined that biofilm-producing bacteria can be 100-10000 times more antibiotic-resistant to planktonic forms [1].

A biofilm is defined as an aggregated community of bacterial cells, encased in an extracellular matrix comprising various types of extracellular polymeric substances. These include exopolysaccharides, proteins, lipids, biosurfactants, and extracellular DNA. Biofilm-producing bacteria exhibit resistance to antimicrobial agents, antibiotics, and harsh environmental conditions due to their protected, sessile state [2]. This biofilm-associated infection affects millions of people worldwide. Previous reports have highlighted the relationship between biofilm formation, antibiotic resistance, and the use of antibiofilm agents to prevent biofilm formation [3]. In recent years, there has been a notable interest in the investigation of natural and synthetic antimicrobial and antibiofilm compounds [4].

It has been documented that the therapeutic effects of plants are due to the synergistic effect of many components rather than a single active ingredient and that they provide a more effective treatment by resisting the resistance of microorganisms that are difficult to kill with antibiotics [5, 6]. This situation leads researchers to search for natural antimicrobial agents obtained from plant extracts [7-9].

The members of the genus Astragalus have a great interest in traditional drugs in Turkish folk medicine. Astragalus is a large genus of vascular plants from the Legominales tribe and Fabaceae family [10]. Astragalus species are a source of polysaccharides, phenolic, and saponins and they are usable for applications in the food, cosmetic, and pharmaceutical industries [11].

The formulation of nanofibres loaded with bioactive ingredients for biomedical purposes has recently attracted a great deal of attention [12,13]. The integration of bioactive components into delivery systems have been modified to facilitate the enhancement of the following qualities: solubility, bioavailability, stability, pharmacological activity, and protection from both physical and chemical degradation. A variety of novel herbal drug delivery systems have been developed recently [14-16]. Electrospinning is a versatile, simple, effective, and widely used technique for generating nanosized fibers [17]. Electrospun nanofibers are used as wound dressings, scaffolds, and drug release systems due to their resemblance to the natural extracellular matrix, high surface area, and improved mechanical performance [18]. The researchers have revealed that nanofibers can be used as drug delivery systems in various disease treatments. Particularly, nanofibers obtained by using the electrostatic spinning method are advantageous in terms of loading the desired amount of drug and controlling the release of hydrophilic drugs. In this study, nanofibers were obtained from polymer blends of polycaprolactone, sericin, and gelatin using electrostrospinning. Polycaprolactone is biocompatible, biodegradable, non-toxic, electrostatic spinnability, and similar to extracellular matrices. This makes them advantageous for nanofiber production. Sericin and gelatin are hydrophilic, biocompatible, important biomaterials that can be used in medical and cosmetic fields [19]. There are a limited number of studies on extract-loaded electrospun nanofibers for biomedical applications [20]. Therefore, it is important to determine the chemical contents and biological activities of plants and reveal their potential for use in biotechnological studies. To the best of our knowledge, no previous investigation has been reported regarding the chemical composition, biological activity, and potential biotechnological applications of Astragalus lusitanicus subsp. orientalis. The objective of this study is to ascertain the chemical composition of the methanol extract from Astragalus lusitanicus subsp. orientalis and to investigate its in vitro antimicrobial and antibiofilm activities, to assess its potential for biotechnological applications.

MATERIALS AND METHODS

Preperation of Methanol Extract

The aerial parts of Astragalus lusitanicus Lam. subsp. orientalis Chater & Meikle were collected during the flowering period from a rocky area alongside the roadside in Sakar Tepe province, Muğla/Turkey (37° 03’ 67” N 28° 21’ 45” E) at an altitude of 450 meters. These collected samples were subjected to drying in a controlled environment with low humidity, good airflow, and protection from direct sunlight, after which they were finely powdered. For the preparation of a methanol extract of A. lusitanicus subsp. orientalis (AL-MeOH), a modified ultrasonic extraction method was employed [21].

Determination of Phenolic Contents of Methanol Extract

The total phenolic and flavonoid contents of the methanol extract were initially determined spectroscopically. Subsequently, the presence of 30 phenolic compounds in the extract was investigated using a previously validated method [22] employing Liquid Chromatography-Electrospray Tandem Mass Spectrometry (LC–ESI–MS/MS).

Fabrication of Electrospun Nanofiber

The electrospinning processes were carried out by the Electrospinning System (Idasonic, Ave Spn L30, Turkey). The electrospinning condition consists of polymer solutions as shown in Table 1. Polycaprolactone (PCL), sericin, gelatin, and all other solvents were purchased from Sigma-Aldrich. In the electrospinning procedure: PCL was dissolved in trifluoroethanol (TFE) and sericin and gelatin

Table 1. Electrospinning conditions and preparation of polymer solutions

Formula code	The concentration of polymer (w/v)	Electrospinning process parameters				
		Flow rate (mL/h)	Voltage (kV)	Spinerette-collector distance (mm)	Drum speed (rpm)	Oscillation range (mm)
N_1	10% PCL, 8% sericin and 5% gelatin (7:2:1)	0.30	20	150	50	15
N_2	10% PCL, 6% sericin and 5% gelatin (7:2:1)	0.25	15	150	50	15
N_3	12% PCL, 8% sericin and 5% gelatin (6:3:1)	0.50	20	150	50	15
N_4	12% PCL, 8% sericin and 5% gelatin (7:2:1)	0.70	15	150	50	15
N_5	12% PCL, 8% sericin and 5% gelatin (7:2:1)	0.30	20	150	50	15
N_6	12% PCL, 8% sericin and 5% gelatin (7:2:1)	0.30	20	100	50	15
N_7	12% PCL, 10% sericin and 5% gelatin (7:2:1)	0.50	15	150	50	15
N_8	12% PCL, 10% sericin and 5% gelatin (7:2:1)	0.50	20	100	50	15

were dissolved in distilled water (dH_2O) by mixing with a magnetic stirrer at 50°C and 35°C, respectively until a homogeneous mixture was obtained [23]. Then polymer blends were prepared (Table 1).

Characterization of Nanofiber Structure

The nanofiber structures' images underwent analysis through scanning electron microscopy (SEM). Before imaging with an LEO 1430 VP SEM (Carl Zeiss AG, Jena, Germany) at an accelerating voltage of 20 kV, the samples underwent sputter-coating with gold for 30 s at 100 mA. The ImageJ program was used to determine the nanofibers' diameters.

For Fourier transform infrared spectroscopy (FTIR) analysis (Perkin Elmer Spectrum Two spectrometer), each sample was pulverized and mixed with potassium bromide (KBr). The suspension was pressed into a transparent pellet and analyzed in absorbance mode within the range of 400-3600 cm^{-1}.

The nanofiber samples were analyzed using a Bruker D8 Advance diffractometer (Cu Kα radiation) with a scanning rate of 0.025°/s over a 2θ range of 2° to 60°, at 30 kV and 40 mA.

Fabrication of *Astragalus Lusıtanıcus* Extracts Loaded Nanofiber

Among the electrospun formulas in Table 1, the N_6 formula was evaluated more suitable formula by SEM analysis therefore, the fabrication of *A. lusitanicus* extracts-loaded nanofiber was carried out with the N_6 formula. The N_6 formula was prepared as shown in Table 1 and 1% *A. lusitanicus* extracts were added polymer solution.

***In Vitro* Release Test**

Firstly, plant extracts were dissolved in phosphate-buffered saline (PBS) at two-fold serial dilutions concentrations (0.78 to 100 mg/mL), and the absorbances were measured with a spectrophotometer at 520 nm and a standard calibration curve was prepared. To examine the release profiles of nanofiber (N_6) and AL-MeOH loaded nanofiber ($N_{6\text{-AL-MeOH}}$), the samples were cut into 1 cm x 1 cm and placed into tubes that contained PBS buffer (pH:7,4) and incubated in a water bath at 37°C. Samples were taken from the medium at certain time intervals (0, 3, 5, 10, 20, 30, 40, 60, 80, 100, and 120 min) and absorbance was measured by spectrophotometer [24].

***In Vitro* Swelling Test**

The dry weight of the N_6 and $N_{6\text{-AL-MeOH}}$ was measured for the determination of swelling (%). The nanofibers were placed in tubes that contained PBS (pH 7.4) and incubated in a water bath at 37 °C. The nanofiber samples were removed from the PBS at specific time intervals (0, 10, 20, 30, 40, 60, 80, 100, 120, 140, 180, and 220 min). Excess water was removed using filter paper, and the samples were reweighed. The percentage swelling of the nanofiber was calculated using equation (1) [25]:

$$Swelling\ (\%) = [(W_w - W_d)/W_d] \times 100 \quad (1)$$

Ww and Wd represent the wet and dry nanofibers weight, respectively.

In Vitro Biodegradation Test

The N_6 and $N_{6\text{-AL-MeOH}}$ samples were cut into 2.5 cm × 2.5 cm pieces. The initial weight of each specimen was measured before being placed in test tubes containing 30 mL of PBS (pH 7) for an *in vitro* degradation study. The tubes were then incubated at 37°C and 150 rpm and observed for 14 days. Triplicate specimens for each sample condition were removed from the tubes at different time intervals. The samples were rinsed with distilled water two to three times and dried using filter paper followed by vacuum for three days. The percentage of nanofiber biodegradation was determined using equation (2) [26]:

$$Biodegradation\ (\%) = [(W_0 - W_1)/W_1] \times 100 \qquad (2)$$

W_1 and W_0 are the weight of samples after degradation and the initial weight before degradation, respectively.

Evaluation of *In Vitro* Antimicrobial Activity

The antimicrobial activities were examined against *Listeria monocytogenes* ATCC 19115, *Staphylococcus aureus* ATCC 25923, *Klebsiella pneumoniae* NRRLB 4420, *Pseudomonas aeruginosa* ATCC 11778, *Bacillus subtilis NRS 744*, *Escherichia coli* ATCC 35218, *Enterococcus faecalis* ATCC 51289, *Escherichia coli* ATCC 25922. Test microorganisms were obtained from the bacterial culture collection of the Faculty of Pharmacy, Afyonkarahisar Health Sciences University (Afyonkarahisar, Turkey), and used in this study. The antimicrobial of AL-MeOH extract was evaluated by disc diffusion and broth microdilution assay [27, 28]. For the broth microdilution test, a stock solution of each extract was diluted in the Mueller Hinton Broth (MHB) in two-fold serial dilutions to obtain concentrations from 1.56 to 100 mg/mL at a total volume of 100 µL per well in 96-well microtiter plates. 100 µL of each pathogen test microorganism was added to each well at a final concentration of 1×10^6 cfu/mL and incubated at 37°C, for 24 h. The medium, 0.1% (w/v) penicillin, and dH_2O were used as the non-treated, positive, and negative controls, respectively.

In disc diffusion assay; bacteria cultured prepared in MHB at 37°C, 24 h, and then its turbidity was adjusted to equal to 0,5 Mc Farland turbidity. 10 µL of each extract (10 mg/mL and 100 mg/mL concentrations of AL-MeOH dropped on sterile discs (zone diameter 6 mm) under aseptic conditions. 0,1 mL of each bacteria culture was spread on Mueller Hinton Agar (MHA) and then discs were placed on petri dishes and incubated at 37°C for 24 h. After the incubation period, inhibition zone diameters were measured and evaluated in comparison with the control group. 10 mg/mL of penicillin G and dH_2O were used as a positive and negative control, respectively. The diameter of growth inhibition zones was measured in millimeters. In addition, N_6 and $N_{6\text{-AL-MeOH}}$ samples were cut into 1 cm × 1 cm pieces and the same procedure was carried out for nanofibers.

Investigation of Antibiofilm Effects Against *Staphylococcus Aureus*

The biofilm inhibition effects of AL-MeOH extract were evaluated by a 3-[4,5-dimethyl-2-thiazolyl]-2, 5-diphenyl-2H-tetrazolium-bromide (MTT) colorimetric method with modification [29]. In this procedure; 1000 µL of each ½ x MIC, MIC, and 2 x MIC concentration of AL-MeOH were added to 24-well microtiter plates. N_6 and $N_{6\text{-AL-MeOH}}$ were cut into 1 x 1 cm pieces and placed into 24-well microtiter plates. Penicillin G (30 mg/mL) was used as the positive control and the medium was used as a negative control. An equal volume of the *S. aureus* ATCC 25923 (1×10^6 cfu/mL) which was determined biofilm producer in the previous study was added to 24-well microtiter plates except in the well with medium alone and incubated at 37°C for 6 and 24 h. The supernatants were discarded, and the cells were washed three times with PBS. Next, 1500 µL of PBS and 500 µL of MTT (0.3%) were added to each well, and the plate was incubated for 2 hours at 37°C. After incubation, the MTT solutions were removed, and 1500 µL of Dimetil sülfoksit (DMSO) and 250 µL of 0.1 M glycine buffer (pH 10.2) were added to each well to dissolve the formazan crystals. The plate was then incubated for 15 minutes at ambient conditions. Finally, the optical density was measured at a wavelength of 570 nm using a microplate spectrophotometer. The experiment was conducted in triplicate. To calculate the percentage of biofilm inhibition, the following equation (3) was used [29].

$$Inhibition\ (\%) = \left[1 - \left(\frac{A_{570} of\ the\ test}{A_{570} of none\ teated\ control}\right)\right] \times 100 \qquad (3)$$

Determination of Biofilm Structure by Scanning Electron Microscope

For this procedure, ½ x MIC, MIC, and 2 x MIC concentrations of AL-MeOH were added to the 24-well flat-bottom plate containing 14 x 14 mm polylysine slides. The N_8 and $N_{8\text{-AL-MeOH}}$ structures were cut into 1 x 1 cm and placed into 24-well microtiter plates. Then 1000 µL of *S. aureus* ATCC 25923 cultures (1×10^6 cfu/mL) were added to 24-well microtiter plates and incubated for 6 and 24 h at 37°C. At the end of the application periods, the incubation was stopped and the materials were left in the primary fixative (2.5% glutaraldehyde solution prepared in PBS) at 4°C for 24 h. The samples were washed three times with PBS for 15 minutes, then removed from the fixative and kept in the dark in the rotator for 1 hour in the secondary fixative containing Osmium tetroxide (OsO_4). Then they were washed with PBS and the samples were dehydrated with ethyl alcohol (50%, 70%, 90%, 95%, and 100%) by Polaron CPD Critical Point Dryer. Finally coated with gold-palladium using the Polaron SC7620 Sputter Coater. The samples were imaged by a SEM. (JEOL JSM-5600LV) [30].

Statistical Analysis

The experiments were performed three times, and the outcomes were presented as the average and standard deviation of three parallel measurements.

RESULTS AND DISCUSSION

Determination of the chemical compositions and biological activities of the medicinal and aromatic plants is very important in terms of revealing their potential to treat various diseases. In addition, these plants can be used together with biotechnological studies to increase their efficiency [31]. Plants are a source of many chemical compounds with antimicrobial activity and the potential to have the potential to treat antimicrobial-resistant infections. In recent years, health concerns related to the side effects of synthetic compounds and the emergence of antibiotic resistance in pathogens have led to the development of electrospinning research towards the development of plant extracts loaded nanofibers [32]. Thus, in the present study, the chemical content and biological activity of the methanol extract of *A. lusitanicus* were determined and plant extract-loaded nanofiber was obtained, successfully. The anti-biofilm effect of plant extract and extract-loaded nanofiber was investigated for the first time. The methanol extract from *A. lusitanicus* subsp. *orientalis* was obtained using ultrasound-assisted extraction, and the extract yield was found to be 8.7%. Subsequently, the total phenolic and flavonoid contents of the methanol extract were determined spectroscopically as 26.5 mg gallic acid equivalents (GAEs)/g and 25.0 mg rutin equivalents (REs)/g, respectively (Figure 1).

To identify and quantify the presence of 30 phytochemicals in the extract, LC–ESI–MS/MS was utilized, and the main components identified were hesperidin, quercetin, and hyperoside (Table 2). Hesperidin was found to be the most abundant compound, with a concentration of 7864 µg/g, followed by quercetin (2223 µg/g) and hyperoside (1804 µg/g).

Table 2. Concentration of selected phenolic compounds in the methanol extract

Compound	Concentration (µg/g extract)
Gallic acid	326 ± 4
Protocatechuic acid	617 ± 7
Pyrocatechol	nd
3,4-Dihydroxyphenylacetic acid	0.96 ± 0.14
(+)-Catechin	nd
2,5-Dihydroxybenzoic acid	11.4 ± 0.5
Chlorogenic acid	244 ± 2
3-Hydroxybenzoic acid	9.16 ± 0.21
4-Hydroxybenzoic	190 ± 1
(-)-Epicatechin	1.76 ± 0.07
Caffeic acid	98.7 ± 0.8
Syringic acid	3.99 ± 0.40
Vanillin	12.1 ± 0.5
Verbascoside	nd
Taxifolin	nd
p-Coumaric acid	71.6 ± 0.6
Sinapic acid	2.49 ± 0.23
Ferulic acid	39.7 ± 1.2
Luteolin 7-glucoside	6.96 ± 0.44
Hesperidin	7864 ± 100
Hyperoside	1804 ± 22
Rosmarinic acid	11.7 ± 2.8
Apigenin 7-glucoside	17.9 ± 0.7
Pinoresinol	14.0 ± 0.5
2-Hydroxycinnamic acid	nd
Eriodictyol	nd
Quercetin	2223 ± 55
Luteolin	0.78 ± 0.03
Kaempferol	85.9 ± 0.4
Apigenin	nd

nd: Not detected.

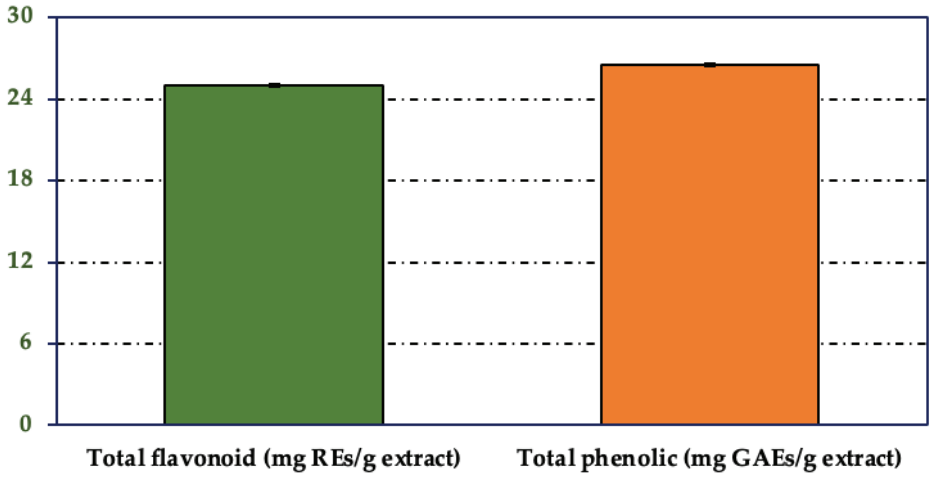

Figure 1. Total phenolic and flavonoid contents of the methanol extract (GAEs and REs: Gallic acid and rutin equivalents, respectively).

The methanol extract exhibited significant levels of total phenolic and flavonoid contents. These findings indicate that the extract possesses a high concentration of phenolic compounds and flavonoids, which are well-known for their potential health benefits. Phenolic compounds and flavonoids are known for their antioxidant properties and have been associated with various biological activities, such as anti-inflammatory, antimicrobial, and anticancer effects [33]. The observed levels of total phenolic and flavonoid content in the methanol extract suggest its potential as a valuable source of natural bioactive compounds, which could be explored for various applications in the fields of pharmaceuticals, nutraceuticals, and functional foods.

The LC-MS/MS analysis revealed the presence of prominent components in the methanol extract including hesperidin, quercetin, and hyperoside. As far as our literature survey could ascertain, no study has been found on the chemical composition of *A. lusitanicus* subsp. *orientalis*. However, there are phytochemical studies conducted on other *Astragalus* species. It has been reported that the methanol extract from the aerial parts of *Astragalus gymnolobus* is rich in hesperidin and hyperoside [34]. Haşimi et al. [35] conducted studies on other *Astragalus* species to identify a total of twenty-four phenolic compounds and three non-phenolic organic acids in three *Astragalus* species, wherein varying amounts of hesperidin and hyperoside were found to be the most abundant flavonoids. Moreover, Sarikurkcu and Zengin [36] detected hyperoside, apigenin, p-coumaric acid, and ferulic acid as the main compounds in different parts of *A. macrocephalus* subsp. *finitimus*. Similarly, Arumugam et al. [37] identified seven phytochemicals (syringe acid, p-coumaric acid, o-coumaric acid, luteolin, ferulic acid, hesperidin, and benzoic acid) in methanolic extracts obtained from various parts of *A. ponticus*. The results of this study are consistent with the literature data regarding the phytochemical composition of *A. lusitanicus* subsp. *orientalis*.

The electrospun nanofibers of PCL/sericin/gelatin, which are biocompatible, biodegradable, and non-toxic, were obtained successfully and AL-MeOH loaded nanofiber was developed for a novel material for biomedical applications such as tissue engineering scaffolds, drug delivery, wound dressings, separation membranes, antibacterial coatings, regenerative medicine, and sensing/biosensing [38].

In this context, the electrospinning parameters, which include flow rate, voltage, spinnerette-collector distance, drum speed, oscillation range, and polymer blending ratio, were optimized. After optimization of conditions, the PCL/chitosan/sericin electrospun nanofiber, which is bead-free fiber with minimum diameter and homogeneously distributed was successfully obtained.

The needle's electrospun parameters were determined as 0.30 mL/h flow rate, 20 kV voltage, 100 mm spinnerette-collector distance, 50 rpm drum speed, 15 mm oscillation range, and a blend of 12% PCL, 8% sericin and 5% gelatin (7:2:1), 1% AL-MeOH were found to be suitable. Polymeric materials, becoming smaller in scale with a large surface area to volume ratio, can provide improved biological properties of plant extracts. The primary advantage of plant-loaded nanofibers is their straightforward production and handling. They can be designed in a variety of sizes and shapes, are easily foldable, cut, shaped, rolled, or stored, and are relatively inexpensive [39].

The images of the SEM analyses of the electrospun nanofibers obtained are shown in Figure 2. The most suitable formula was determined as the N_6 formula, which has the lowest average fiber diameter, the most uniform morphological structure, and no beads structure observed (Table 1). The fiber diameter of N_6 was determined as average 110-150 nm.

AL-MeOH-loaded nanofiber was carried out with the N_6 formula and $N_{6\text{-AL-MeOH}}$ is shown in Figure 3. The fiber diameter of $N_{6\text{-Al-MeOH}}$ was determined as an average of 110-200 nm.

The N_6 possesses the features of being a nanosized and thin fiber structure with a smooth surface. Due to the incorporation of AL-MeOH, the formation of branching of fiber structure increased and the uniform fiber surface seems it did not change the fiber diameter of the $N_{6\text{-AL-MeOH}}$ nanofiber, significantly. The bioactive compounds present in the AL-MeOH extract occupied the porous surface of the electrospun nanofiber [20]. The diameter of $N_{6\text{-AL-MeOH}}$ has been slightly increased due to swelling. It is concluded that the morphology of the nanofibers was slightly affected by the plant extract.

The FTIR spectrum of N_6 and $N_{6\text{-AL-MeOH}}$ nanofibers are shown in Figure 4. The FTIR spectrum presents several bands at curve regions from about 3000 to 400 cm^{-1}. The bands observed at approximately 1600, 1300, and 1100 cm^{-1} in the FTIR spectrum are attributed to an aliphatic C-H, amide I (NH deformation–$NHCOCH_3$), amide II, amide III, and C-O vibrational tensional bonds, respectively. The spectrum of pure PCL nanofibers displays a prominent C=O (carbonyl) stretching band at 1723 cm^{-1}, a characteristic peak that can be observed in the spectra of other PCL-related compounds. We can observe bands corresponding to N_6 when analyzing the $N_{6\text{-AL-MeOH}}$ curve, which is indicative of the lack of any chemical reactions between extracts and polymers.

XRD patterns of N_6 and $N_{6\text{-AL-MeOH}}$ nanofibers are shown in Figures 5 and 6. According to the test result, there was a significant weakening of characteristic peaks of PCL at 20-23°. As can be noted, there are two distinct peaks in the PCL curve; by observing the XRD pattern, the loading of AL-MeOH extract into the PCL nanofiber has been verified.

The XRD of N_6 nanofibers (Fig. 5) shows peaks at 20-23° indicating the crystallinity of the PCL nanofibers. The increase in intensity indicates the increased degree of crystallinity. The XRD pattern implies that the AL-MeOH was successfully loaded in nanofiber.

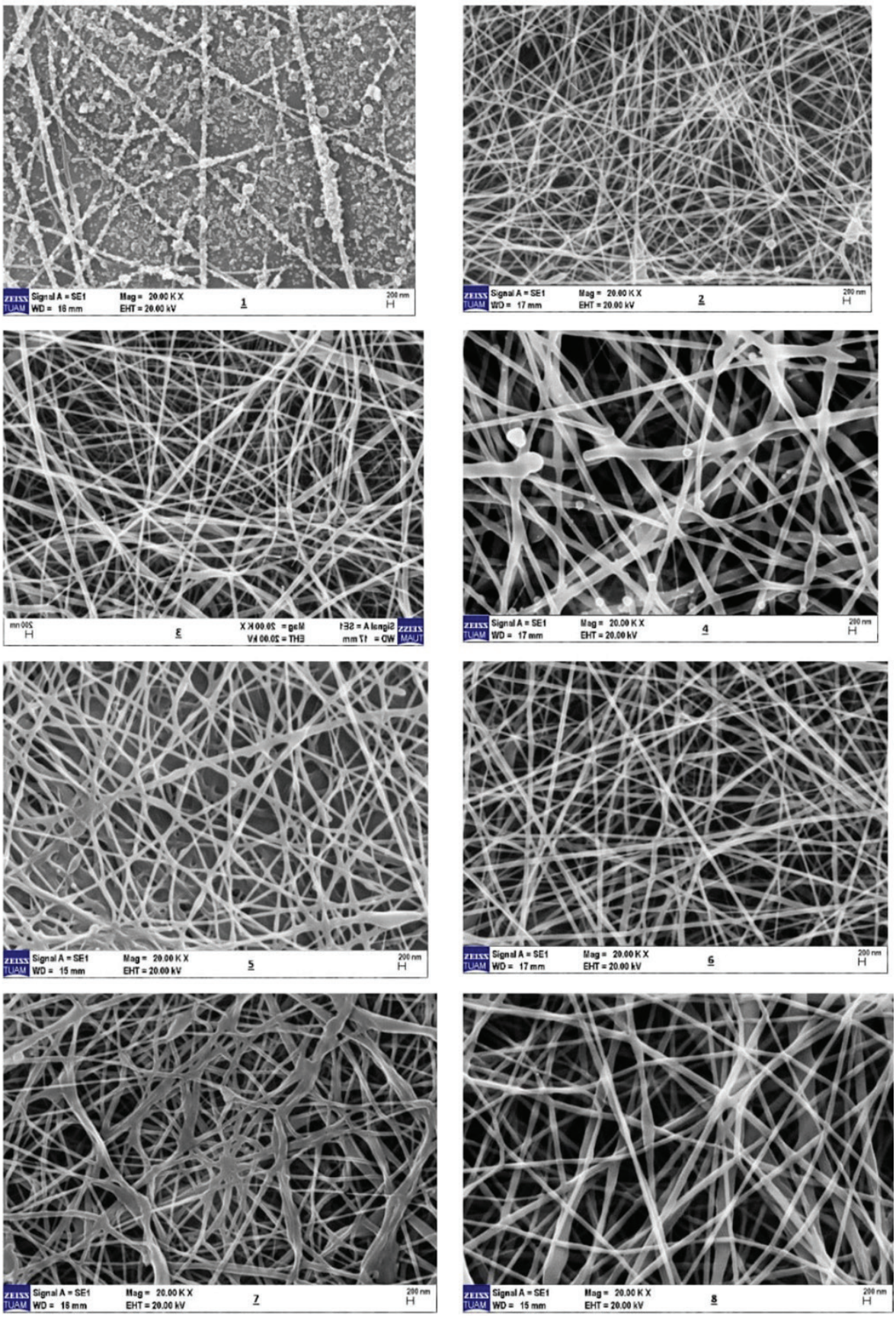

Figure 2. The images of the SEM analysis of the electrospun N_1-N_8 nanofibers (Table 1).

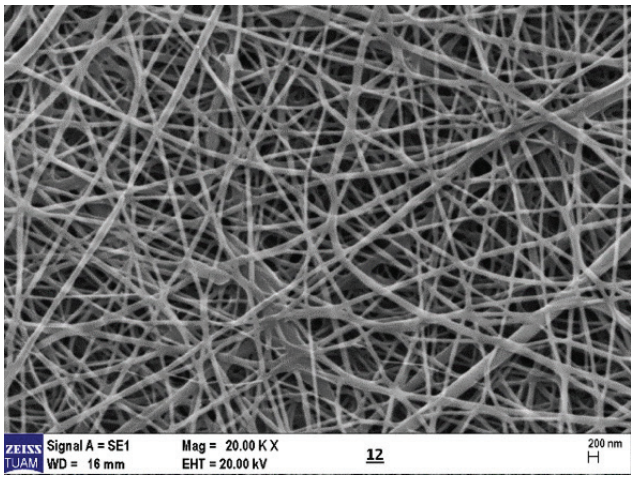

Figure 3. The SEM image of $N_{6\text{-AL-MeOH}}$.

Also in this study, N_6 and $N_{6\text{-AL-MeOH}}$ nanofibers were analyzed for *in vitro* swelling, extract release, and biodegradation tests. The wettability rate of nanofibers increased rapidly in the 20 minutes then the swelling rate of nanofibers increased more slowly and the swelling rate was fixed in 140-220 min (Fig. 7).

The swelling behavior of nanofibres is a crucial aspect of biomedical applications. The percentage of swelling in nanofibrous scaffolds is highly dependent on their porosity and surface area. The $N_{6\text{-AL-MeOH}}$ nanofiber showed about 89% of swelling behavior, which slightly increased when compared with N_6 nanofiber (67%). Generally, the water-absorbing capability is directly related to the sample's hydrophilicity, surface property, and porosity. In this case, sericin, and gelatin are hydrophilic and PCL is less

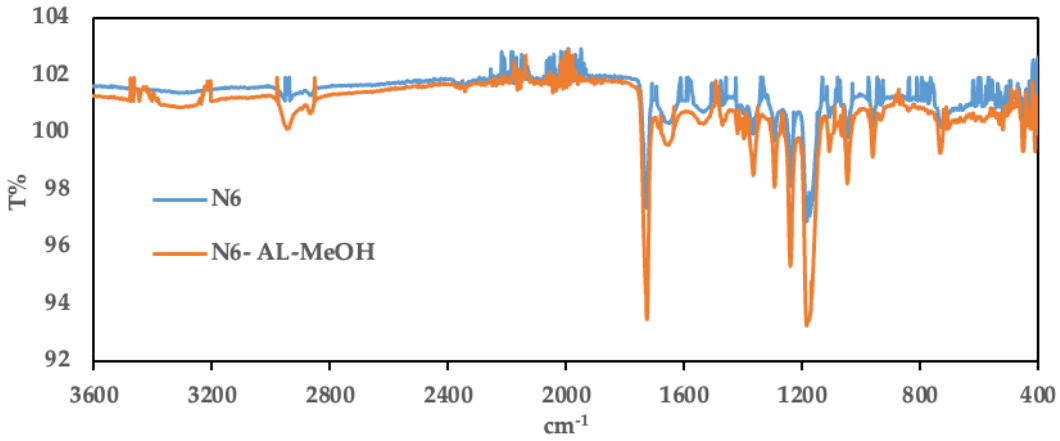

Figure 4. The FTIR spectra of N_6 and $N_{6\text{-AL-MeOH}}$.

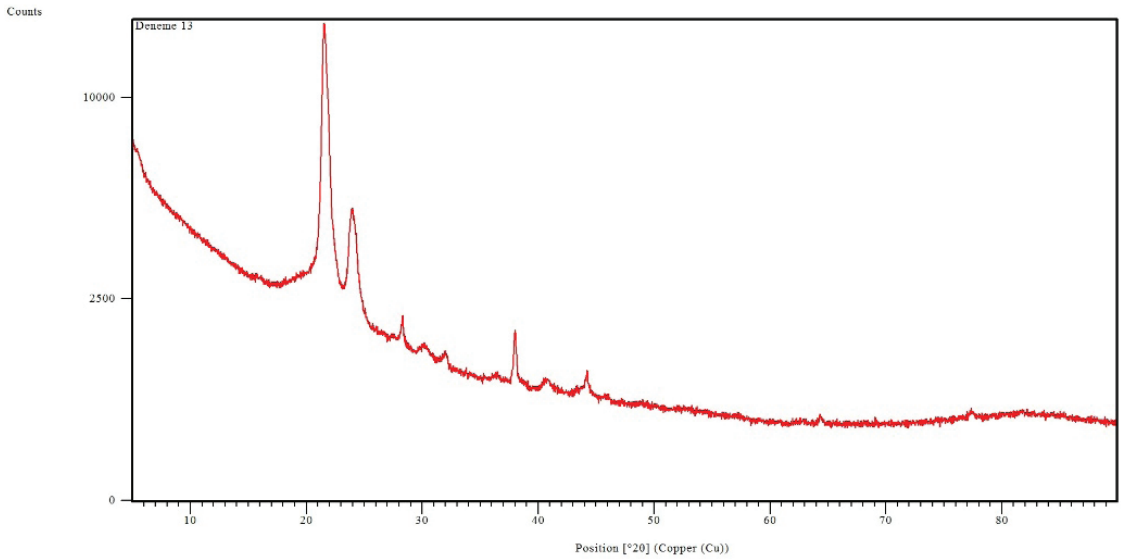

Figure 5. XRD pattern of N_6 nanofiber.

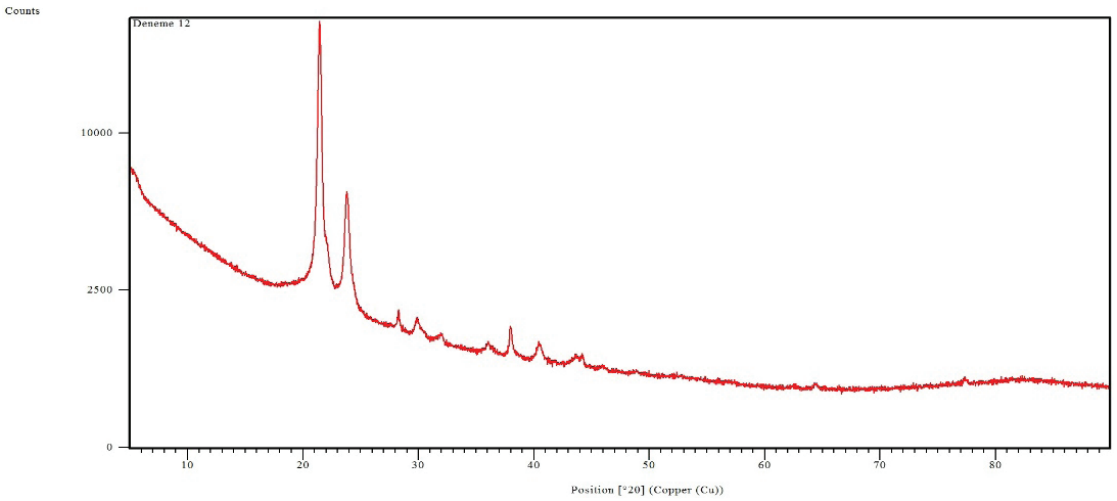

Figure 6. XRD pattern of $N_{6\text{-AL-MeOH}}$ nanofiber.

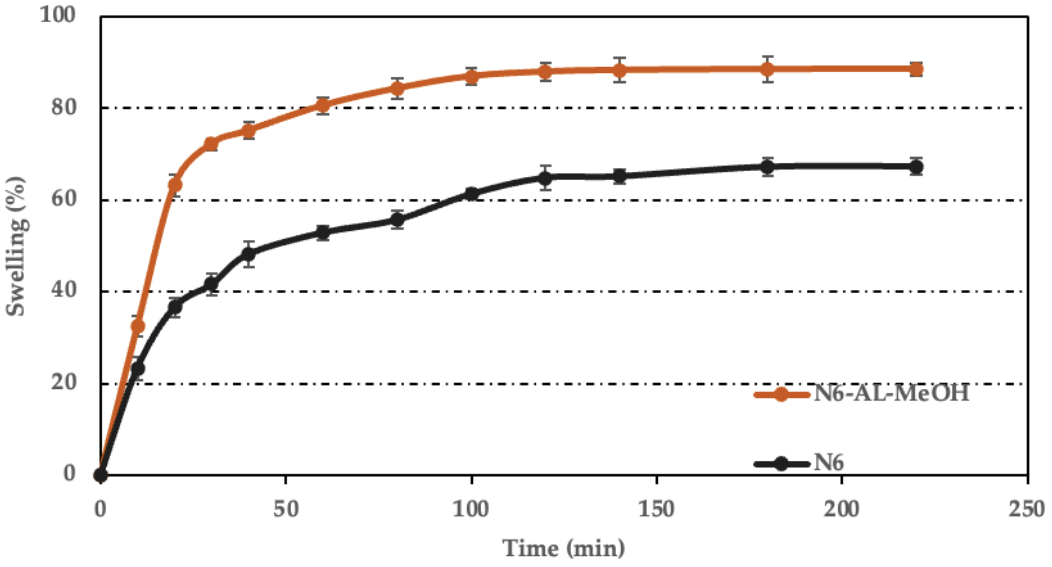

Figure 7. The results of the swelling ratios of nanofibers.

hydrophilic, though $N_{6\text{-AL-MeOH}}$ nanofiber has shown an increased swelling percentage.

The *in vitro* extract release was calculated using the standard calibration curve (R^2 = 0.9781). The rapid release of the extract of $N_{6\text{-AL-MeOH}}$ was determined for 40 minutes then it decreased (Fig. 8). The continuous plant extract release indicates that this nanofiber could be used in pathogen test microorganisms.

According to the *in vitro* biodegradation analysis, N_6, and $N_{6\text{-AL-MeOH}}$ nanofiber biodegraded 29.5% and 38.91%, respectively for the 14th day (Fig. 9)

The $N_{6\text{-AL-MeOH}}$ nanofiber shows progressive weight loss probably due to the hydrophilicity that will contact easily with PBS and degrade faster if the same conditions exist.

The results of *in vitro* extract release test the rapid release of extract of $N_{6\text{-AL-MeOH}}$ was determined for 40 minutes then it decreased. It can be seen that the N_6 and $N_{6\text{-AL-MeOH}}$ nanofibers have almost certainly constant weight because of their very slow degradation rate of 29.5% and 38.91%, respectively for the 14th day.

Al-Kaabi et al. [31] developed electrospun/polycaprolactone nanofibers loaded with *Inula graveolens* extract, which exhibit potential for biomedical applications. Another study by Suryamathi et al. [20] focused on the development of a novel wound dressing material using electrospun PCL nanofibers loaded with *Tridax procumbens* extracts. The findings from these studies support the notion that such scaffolds have the potential to enhance wound healing and

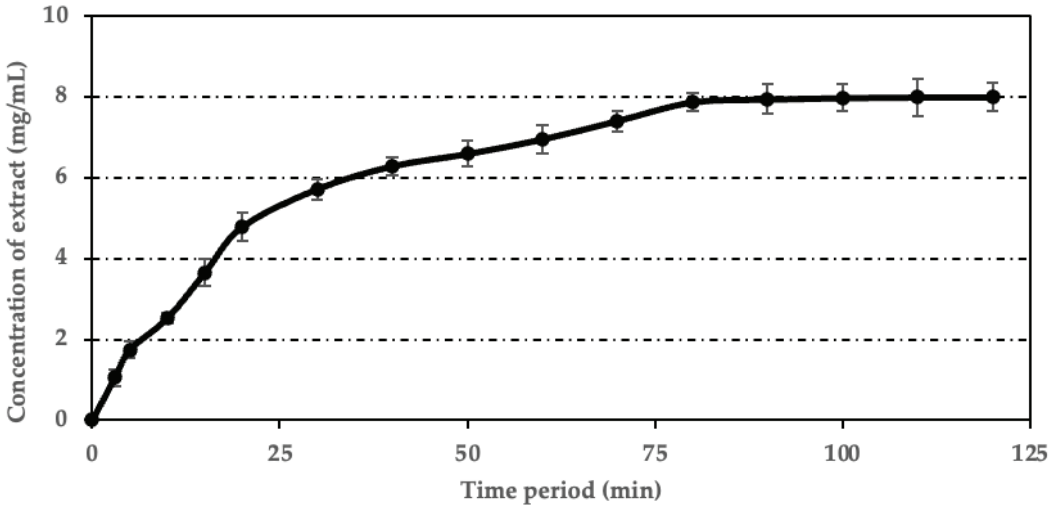

Figure 8. *In vitro* extract release of $N_{6\text{-AL-MeOH}}$.

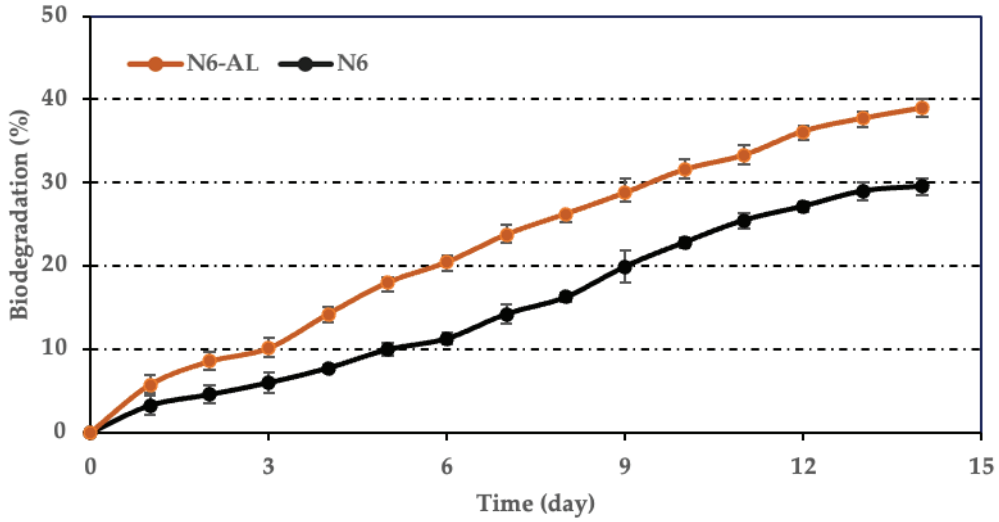

Figure 9. Biodegradation of N_6 and $N_{6\text{-AL-MeOH}}$ nanofibers.

effectively address surfaces contaminated with pathogenic microorganisms, especially within hospital environments.

In this study, MIC values of AL-MeOH against pathogenic test microorganisms were determined and are given in Table 3. The MIC value of AL-MeOH was determined as 50 mg/mL against *S. aureus* ATCC 25923 and, it was determined as 6.25 mg/mL against *E. faecalis* ATCC 51289, *P. aeruginosa* ATCC 11778, *E. coli* ATCC 35218, *E. coli* ATCC 25922, *B. subtilis* NRS 744. In addition, it was determined as 3.12 mg/mL against *L. monocytogenes* ATCC 19115 and *K. pneumoniae* NRRLB 4420.

In addition, the antimicrobial effect of AL-MeOH on pathogen test microorganisms was determined by disc diffusion assay and is shown in Table 4. It was determined that there was an increase in antimicrobial activity in parallel

Table 3. MIC values of AL-MeOH against pathogenic test microorganisms

Pathogen Test Microorganisms	MIC values of AL-MeOH (mg/mL)
L. monocytogenes ATCC 19115	3.12
S. aureus ATCC 25923	50.00
K. pneumoniae NRRLB 4420	3.12
P. aeruginosa ATCC 11778	6.25
E. faecalis ATCC 51289	6.25
E. coli ATCC 35218	6.25
B. subtilis NRS 744	6.25
E. coli ATCC 25922	6.25

Table 4. The results of the disc diffusion assay

Pathogen Test Microorganisms	NC	PC	N6	N6-AL-MeOH	AL-MeOH (10 mg/mL)	AL-MeOH (100 mg/mL)
L. monocytogenes ATCC 1911	-	25±0.00	10±0.25	15±0.50	12±0.25	19±1.22
S. aureus ATCC 25923	-	29±0.95	12±0.20	19±0.75	-	14±0.00
K. pneumoniae NRRLB 4420	-	30±1.25	11±0.50	17±1.00	14±0.50	24±1.25
P. aeuruginosa ATCC 11778	-	29±1.50	14±0.50	20±0.50	13±0.50	22±0.55
E. faecalis ATCC 51289	-	30±0.55	10±0.30	19±0.75	13±0.25	21±0.72
E. coli ATCC 35213	-	30±1.52	12±0.20	17±0.50	11±0.75	18±0.5
E. coli ATCC 25922	-	31±1.75	11±0.25	16±0.50	14±0.85	21±1.47
B. subtilis NRS 744	-	30±0.75	9±0.50	15±0.75	10±0.25	15±1.25

PC: Penicilin G (10 mg/mL). NC dH_2O. Resistant ≤ 14. Moderate 15-18. Sensitive ≥ 19

with the increase in the concentration of plant extracts. The results of zone diameters of the disk diffusion test evaluated as resistant ≤ 14, moderately sensitive 15-18, and susceptible ≥19 mm. The highest antimicrobial activity (24±1.25) was found in 100 mg/mL concentration of AL-MeOH against *K. pneumoniae* NRRLB 4420. *P. aeruginosa* ATCC 11778, *E. faecalis* ATCC 51289, *E. coli* ATCC 35213, *E. coli* ATCC 25922 were determined to be sensitive to 100 mg/mL Al-MeOH. *S. aureus* ATCC 25923 and *B. subtilis* NRS 744 were found to be resistant. All test microorganisms were found resistant to N_6 nanofiber. *S. aureus* ATCC 25923, and *E. faecalis* ATCC 51289 were determined as sensitive and the other microorganisms were found to moderate for $N_{6\text{-AL-MeOH}}$.

The results of the biofilm inhibitions of *S. aureus* ATCC 25923 are shown in Figure 10. The most effective $N_{6\text{-AL-MeOH}}$ group was determined as 96% inhibition for biofilm inhibitions of *S. aureus* ATCC 25923. Following this 2 x MIC of the AL-MeOH group was determined 82% biofilm inhibition.

The images of the biofilm structure are shown in Figure 11. It was determined that the bacteria were attached to the N_6 nanofiber and did not form a biofilm structure but the $N_{6\text{-AL-MeOH}}$ nanofiber was not attached for the 6th and 24th h.

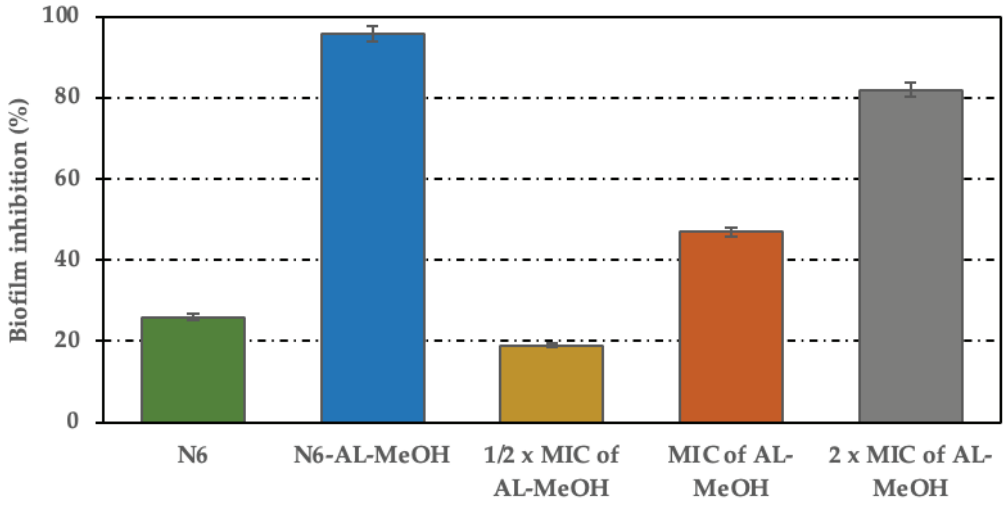

Figure 10. Biofilm inhibition of *Staphyllococcus aureus* ATCC 25923.

Akpınar et al. [40] investigated the antibacterial and antibiofilm activity of cinnamaldehyde-poly (lactic acid)/gelatin electrospun nanofibers. The antibacterial activity of the PLA-Gel-CA nanofibers against *S. aureus* and *P. aeruginosa*, along with their antibiofilm activity against *P. aeruginosa*, were evaluated. PLA-Gel-CA3 nanofibers demonstrated notable antibacterial efficacy against *S. aureus* (31.0 ± 1.20 mm) and *P. aeruginosa* (16.0 ± 1.20 mm), along with a significant inhibition of *P. aeruginosa* biofilm formation by 72.2%. These findings indicate the potential of cinnamaldehyde-loaded nanofibers for wound application owing to their antibacterial and antibiofilm activity, as well as their rapid dissolution characteristics.

The application of ½ x MIC of the AL-MeOH group the structural integrity of bacterial cells is preserved for 6th h but it was determined that the bacterial cell morphology was disrupted, the cells shriveled and there was biofilm inhibition for 24th h. It was determined that the cells were damaged and the cavity formation, fusion of cells, and biofilm inhibition occurred in the treatment of MIC of the AL-MeOH group for 6th h. In addition, it was determined that this situation increased even more, cellular structures were disrupted and cytoplasm loss was observed in the cell at the 24th h. The application of 2 x MIC concentration of the AL-MeOH group resulted in a decrease in the number of cells, disruption of structural integrity, cell fusion, and inhibition of biofilm formation at the 6th h. Moreover, this effect intensified, leading to complete deterioration and indistinguishability of cellular structures. In contrast, the control group exhibited a well-preserved biofilm structure in the exopolysaccharide layer at the 6th hour, and a dense biofilm structure with cell adhesion was observed at the 24th hour.

Bacterial infections are a leading cause of morbidity and mortality worldwide. Significant progress is being made in microbiological research to control many diseases caused by infectious organisms. The MIC value of AL-MeOH determined against pathogen test microorganisms and antibacterial activity has been studied by the disc diffusion assay. In addition, it is generally desired that biomedical materials have antimicrobial properties against bacterial infections. Therefore, the antimicrobial effect of N_6 and $N_{6\text{-AL-MeOH}}$ nanofibers was tested by disc diffusion test. According to the test results, the highest antimicrobial activity was found in 100 mg/mL concentration of AL-MeOH against *K. pneumoniae* NRRLB 4420. *P. aeruginosa* ATCC 11778, *E. faecalis* ATCC 51289, *E. coli* ATCC 35213, and *E. coli* ATCC 25922 were determined to be sensitive to 100 mg/mL AL-MeOH. *S. aureus* ATCC 25923 and *B. subtilis* NRS 744 were found to be resistant. In the present study, antibiofilm activities of Al-MeOH, N_6, and $N_{6\text{-AL-MeOH}}$ nanofibers were tested against biofilm producer *S. aureus* ATCC 25923. Antibiofilm test results revealed that the $N_{6\text{-AL-MeOH}}$ and 2 x MIC concentration of the AL-MeOH group were determined as 96% and 82% biofilm inhibition, respectively.

The researchers have demonstrated a relationship between polyphenols of plant extract with anti-inflammatory, antimicrobial, and antioxidant activity and they stimulate the proliferation and migration of fibroblast cells [30, 41]. It was suggested that a bioactive substance is responsible for the antimicrobial properties of AL-MeOH extracts. Although the exact mechanisms of its antibacterial action are not fully known, several mechanisms have been proposed, including activation of the host immune system, rupture of bacterial membranes, and microbial enzyme interference [42]. According to the SEM images of the biofilm structure, bacteria were attached to the N_6 nanofiber and did not form a biofilm structure but the N_6-AL-MeOH nanofiber was not attached for the 6th and 24th h. The application of extract groups the structural integrity of bacterial cells bacterial cell morphology was disrupted and shriveled depending on the concentration rate. It was determined that the cells were damaged and the cavity formation, fusion of cells, and biofilm inhibition occurred in the treatment of MIC and 2x MIC of the AL-MeOH group. In addition, it was determined that this situation increased even more, cellular structures were disrupted and cytoplasm loss was observed in the cell at the 24th h. The application of 2 x MIC of the AL-MeOH group was observed which decreased the number of cells, disruption of structural integrity, the fusion of cells, and inhibition of biofilm for 6th h, and this situation increased, cellular structures completely deteriorated and became indistinguishable. When the control group was evaluated, a very well-preserved biofilm structure was observed in the exopolysaccharide layer.

In a previous study, Hadisi et al. [43] investigated electrospun gelatin-oxidized starch nanofibres containing henna extract for the treatment of second-degree burn wounds This study demonstrated that the antimicrobial activity of the nano matrix can be attributed in part to the presence of various phenolic compounds, such as 2-hydroxy-1,4-naphthoquinone, in the henna extract, which can interact with the bacterial cell wall and inactivate its function, thus inhibiting microbial growth. Furthermore, other studies have demonstrated the efficacy of chemical compounds in inhibiting biofilm formation [4]. The antimicrobial and antioxidant status of four *Astragalus* species were determined [44]. Based on the results of the study, the extracts exerted moderate antioxidant and reducing activity with low phenolic content. The major constituent of the extracts was determined to be ferulic acid. The extracts did not show any antibacterial activity except *P. aeruginosa*. In another study, Adeli-Sardou et al. [45] investigated the antibacterial and antibiofilm effects of electrospun PCL/gelatin/lawsone nanofibres against biofilm-producing bacteria. The results of the study demonstrated the favorable antibacterial and antibiofilm properties of lawsone-containing scaffolds. Similarly, the results of the present study demonstrated that AL-MeOH, when loaded into a nanofiber, had a marked effect on biofilm inhibition. The findings of the present study indicate that the antimicrobial activity of the

Name	Application Time	
	6 h	24 h
N_6	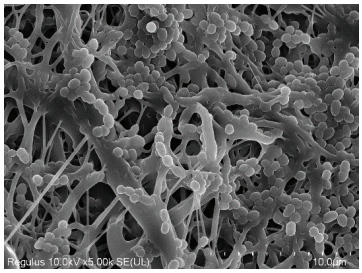	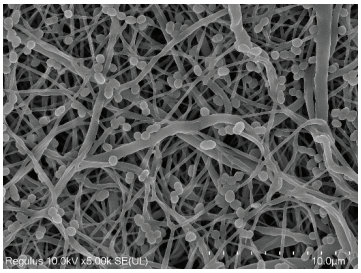
N_6-AL	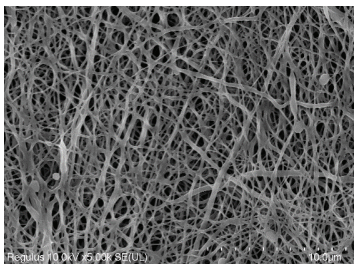	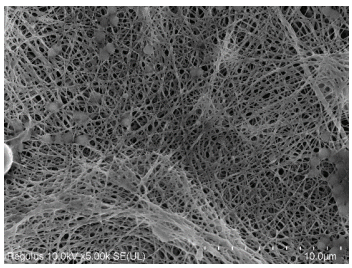
AL-MeOH (1\2 x MIC)	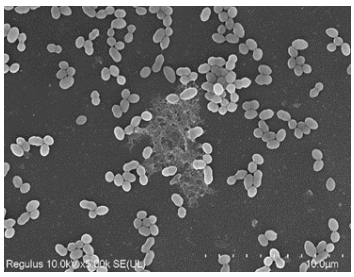	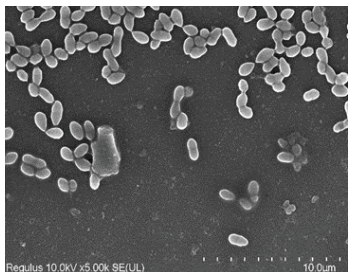
AL-MeOH (MIC)	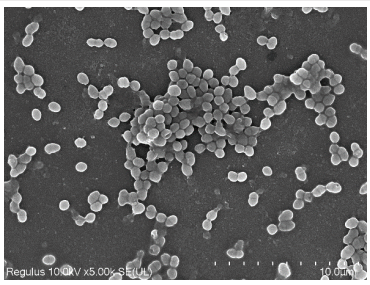	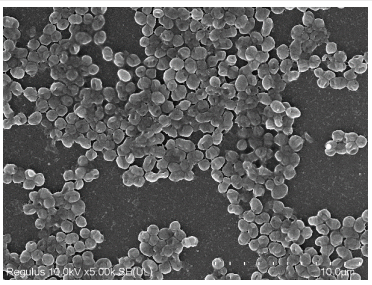
AL-MeOH (2 x MIC)	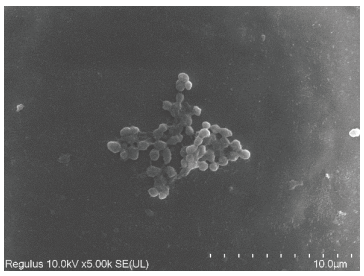	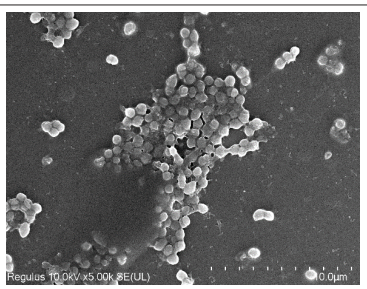
Control	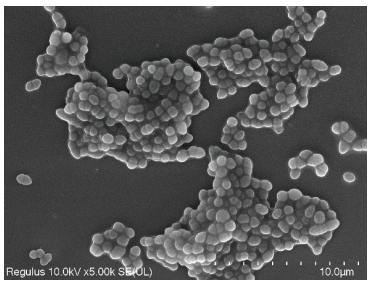	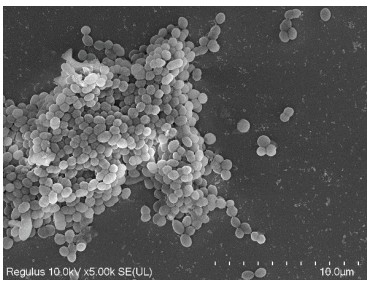

Figure 11. SEM images of antibiofilm assay against *S. aureus* ATCC 25923 at 6 and 24 h.

nanofiber can be attributed, to the presence of various phenolic compounds such as hesperidin, quercetin, and hyperoside in the AL-MeOH. These compounds are capable of interacting with the bacterial cell wall, thereby inactivating its function and inhibiting microbial growth.

CONCLUSION

Astragalus lusitanicus subsp. *orientalis* plant extract's therapeutic potential in biofilm-associated infections has not yet been explored. To our knowledge, this is the first report on the biological and chemical study of *A. lusitanicus* subsp. *orientalis*. Hesperidin, quercetin, and hyperoside were determined as the major constituents of plant extract. Polycaprolactone/sericin/gelatin and plant extract-loaded nanofibers were developed using an electrospinning technique. Characterization analyses and the *in vitro* swelling, biodegradation, and extract release assays revealed that nanofiber and plant extract-loaded nanofiber are useful the biomedical applications. Both plant extract and extract-loaded nanofiber showed antimicrobial activity against pathogen test microorganisms. The results showed that the nanofibres loaded with the plant extract and the plant extract exhibited strong biofilm inhibition of 96% and 82%, respectively. Additionally, the results of this work indicate that the nanofibers act as promising agents for enhancing wound healing and treating surfaces contaminated with pathogenic microorganisms. Consequently, this study holds promise for the development of novel materials with potential antimicrobial properties derived from natural sources, thereby offering potential biomedical applications. Further studies are required to identify the active compounds responsible for the observed antimicrobial activity.

ACKNOWLEDGEMENTS

The authors would like to thank to Dr. Olcay Ceylan for his kind help in identifying the plant materials used in this study.

AUTHORSHIP CONTRIBUTIONS

Authors equally contributed to this work.

DATA AVAILABILITY STATEMENT

The authors confirm that the data that supports the findings of this study are available within the article. Raw data that support the finding of this study are available from the corresponding author, upon reasonable request.

CONFLICT OF INTEREST

The author declared no potential conflicts of interest with respect to the research, authorship, and/or publication of this article.

ETHICS

There are no ethical issues with the publication of this manuscript.

STATEMENT ON THE USE OF ARTIFICIAL INTELLIGENCE

Artificial intelligence was not used in the preparation of the article.

REFERENCES

[1] Hall-Stoodley L, Costerton JW, Stoodley P. Bacterial biofilms: from the natural environment to infectious diseases. Nat Rev Microbiol 2004;2:95–108. [CrossRef]

[2] DeLeon S, Clinton A, Fowler H, Everett J, Horswill AR, Rumbaugh KP. Synergistic interactions of Pseudomonas aeruginosa and Staphylococcus aureus in an in vitro wound model. Infect Immun 2014;82:4718–4728. [CrossRef]

[3] Shakibaie M, Forootanfar H, Golkari Y, Mohammadi-Khorsand T, Shakibaie MR. Anti-biofilm activity of biogenic selenium nanoparticles and selenium dioxide against clinical isolates of Staphylococcus aureus, Pseudomonas aeruginosa, and Proteus mirabilis. J Trace Elem Med Biol 2015;29:235–241. [CrossRef]

[4] Ahire JJ, Hattingh M, Neveling DP, Dicks LMT. Copper-containing anti-biofilm nanofiber scaffolds as a wound dressing material. PLoS One 2016;11:e0152755. [CrossRef]

[5] Sree KS, Yasodamma N, Chinthala P. Phytochemical screening and in vitro antibacterial activity of the methanolic leaf extract: Sebastiania chamaelea Muell. Bioscan 2010;5:173–175.

[6] Nazri NM, Ahmat N, Adnan A, Mohamad SS, Ruzaina SS. In vitro antibacterial and radical scavenging activities of Malaysian table salad. Afr J Biotechnol 2011;10:5728–5735.

[7] Dash BK, Sultana S, Sultana N. Antibacterial activities of methanol and acetone extracts of fenugreek (Trigonella foenum) and coriander (Coriandrum sativum). Life Sci Med Res 2011;27:1–8.

[8] Saddiqe Z, Naeem I, Maimoona A. A review of the antibacterial activity of Hypericum perforatum L. J Ethnopharmacol 2010;131:511–521. [CrossRef]

[9] Snoussi M, Ahmad I, Aljohani AMA, Patel H, Abdulhakeem MA, Alhazmi YS, et al. Phytochemical analysis, antioxidant, and antimicrobial activities of Ducrosia flabellifolia: A combined experimental and computational approaches. Antioxidants (Basel) 2022;112174. [CrossRef]

[10] Li X, Qu L, Dong Y, Han L, Liu E, Fang S, et al. A review of recent research progress on the Astragalus genus. Molecules 2014;19:18850–18880. [CrossRef]

[11] Hamedi A, Yousefi G, Farjadian S, Bour Bour MS, Parhizkar E. Physicochemical and immunomodulatory properties of gum exudates obtained from Astragalus myriacanthus and some of its isolated carbohydrate biopolymers. Iran J Pharm Res 2017;16(4):1520-1530.

[12] El-Naggar ME, Abdelgawad AM, Abdel-Sattar R, Gibriel AA, Hemdan BA. Potential antimicrobial and antibiofilm efficacy of essential oil nanoemulsion loaded polycaprolactone nanofibrous dermal patches. Eur Polym J 2023;184:111782. [CrossRef]

[13] Ndlovu SP, Motaung K, Adeyemi SA, Ubanako P, Ngema L, Fonkui TY, et al. Sodium alginate-based nanofibers loaded with Capparis sepiaria plant extract for wound healing. J Biomater Sci Polym Ed 2024;35:2380-2401. [CrossRef]

[14] Di Salle A, Viscusi G, Di Cristo F, Valentino A, Gorrasi G, Lamberti E, et al. Antimicrobial and antibiofilm activity of curcumin-loaded electrospun nanofibers for the prevention of the biofilm-associated infections. Molecules 2021;26:4866. [CrossRef]

[15] Hamidi E, Alhaloush R, Şenol Ş, Akyol E. An overview on current trends and future outlook of hydrogels in drug delivery. Sigma J Eng Nat Sci 2023;41:1047–1061. [CrossRef]

[16] Kaya S, Derman S. Production, characterization and antioxidant activity evaluation of quercetin loaded PLGA nanofibers. Sigma J Eng Nat Sci 2022;40:433–440.

[17] Roshanfar F, Hesaraki S, Dolatshahi-Pirouz A. Electrospun silk fibroin/kappa-carrageenan hybrid nanofibers with enhanced osteogenic properties for bone regeneration applications. Biology (Basel) 2022;11. [CrossRef]

[18] Schiffman JD, Schauer CL. One-step electrospinning of cross-linked chitosan fibers. Biomacromolecules 2007;8:2665–2667. [CrossRef]

[19] Arun A, Malrautu P, Laha A, Ramakrishna S. Gelatin nanofibers in drug delivery systems and tissue engineering. Eng Sci 2021;16:71–81.

[20] Suryamathi M, Ruba C, Viswanathamurthi P, Balasubramanian V, Perumal P. Tridax procumbens extract loaded electrospun PCL nanofibers: A novel wound dressing material. Macromol Res 2019;27:55–60. [CrossRef]

[21] Latiff NA, Ong PY, Abd Rashid SNA, Abdullah LC, Mohd Amin NA, Fauzi NAM. Enhancing recovery of bioactive compounds from Cosmos caudatus leaves via ultrasonic extraction. Sci Rep 2021;11:17297. [CrossRef]

[22] Cittan M, Çelik A. Development and validation of an analytical methodology based on liquid chromatography–electrospray tandem mass spectrometry for the simultaneous determination of phenolic compounds in olive leaf extract. J Chromatogr Sci 2018;56:336–343. [CrossRef]

[23] Erdoğmuş SF, Altıntaş ÖE, Çelik S. Production of fungal chitosan and fabrication of fungal chitosan/polycaprolactone electrospun nanofibers for tissue engineering. Microsc Res Tech 2023;86:1309–1321. [CrossRef]

[24] Cesur S. Production of gentamycin-loaded Poly(Vinyl Alcohol)/Gelatin nanofiber by electrospinning method as wound dressing material. Konya Muhendislik Bilim Derg 2022;10:878–888. [Turkish] [CrossRef]

[25] Ahamed N, Sastry T. Wound dressing application of chitosan based bioactive compounds. Int J Pharm Life Sci 2011;2:991–996.

[26] Kim K, Yu M, Zong X, Chiu J, Fang D, Seo YS, et al. Control of degradation rate and hydrophilicity in electrospun non-woven poly(d,l-lactide) nanofiber scaffolds for biomedical applications. Biomaterials 2003;24:4977–4985. [CrossRef]

[27] Clinical and Laboratory Standards Institute. Methods for Dilution Antimicrobial Susceptibility Tests for Bacteria That Grow Aerobically; Approved Standard. 7th ed. Wayne, PA: Clinical and Laboratory Standards Institute; 2006.

[28] Clinical and Laboratory Standards Institute. Performance Standards for Antimicrobial Susceptibility Testing. 26th ed. Wayne, PA: Clinical and Laboratory Standards Institute; 2016.

[29] Erdoğmuş SF, Bilecen C, Erdal Altıntaş Ö, Ulukütük S, Kargıoğlu M. The antibiofilm effects of some Cistus spp. against pathogenic microorganisms. Int J Plant Based Pharm 2022;2:252–260. [CrossRef]

[30] Fernandes FHA, Salgado HRN. Gallic acid: Review of the methods of determination and quantification. Crit Rev Anal Chem 2016;46:257–265. [CrossRef]

[31] Al-Kaabi WJ, Albukhaty S, Al-Fartosy AJM, Al-Karagoly HK, Al-Musawi S, Sulaiman GM, et al. Development of Inula graveolens (L.) plant extract electrospun/polycaprolactone nanofibers: A novel material for biomedical application. Appl Sci 2021;11:828. [CrossRef]

[32] Zhang W, Ronca S, Mele E. Electrospun nanofibres containing antimicrobial plant extracts. Nanomaterials (Basel) 2017;7:42. [CrossRef]

[33] Rathod NB, Elabed N, Punia S, Ozogul F, Kim SK, Rocha JM. Recent developments in polyphenol applications on human health: A review with current knowledge. Plants (Basel) 2023;12:1217. [CrossRef]

[34] Sarikurkcu C, Sahinler SS, Tepe B. Astragalus gymnolobus, A. leporinus var. hirsutus, and A. onobrychis: Phytochemical analysis and biological activity. Ind Crops Prod 2020;150:112366. [CrossRef]

[35] Haşimi N, Ertaş A, Yılmaz MA, Boğa M, Temel H, Demirci S, et al. LC-MS/MS and GC-MS analyses of three endemic Astragalus species from Anatolia towards their total phenolic-flavonoid contents and biological activities. Biol Divers Conserv 2017;10:18–30.

[36] Sarikurkcu C, Zengin G. Polyphenol profile and biological activity comparisons of different parts of Astragalus macrocephalus subsp. finitimus from Turkey. Biology (Basel) 2020;9:23. [CrossRef]

[37] Arumugam R, Kirkan B, Sarikurkcu C. Phenolic profile, antioxidant and enzyme inhibitory potential of methanolic extracts from different parts of Astragalus ponticus Pall. S Afr J Bot 2019;120:268-273. [CrossRef]

[38] dos Santos DM, Correa DS, Medeiros ES, Oliveira JE, Mattoso LHC. Advances in functional polymer nanofibers: From spinning fabrication techniques to recent biomedical applications. ACS Appl Mater Interfaces 2020;12:45673-45701. [CrossRef]

[39] Yin K, Divakar P, Wegst UGK. Plant-derived nanocellulose as structural and mechanical reinforcement of freeze-cast chitosan scaffolds for biomedical applications. Biomacromolecules 2019;20:3733-3745. [CrossRef]

[40] Akpınar Z, Ulusoy S, Akgün M, Oral A, Suner SC. Cinnamaldehyde-poly (lactic acid)/gelatin nanofibers exhibiting antibacterial and antibiofilm activity. Int J Polym Mater Polym Biomater 2024;74:998–1007. [CrossRef]

[41] Vittorazzi C, Endringer D, Andrade T, Scherer R, Fronza M. Antioxidant, antimicrobial and wound healing properties of Struthanthus vulgaris. Pharm Biol 2015;54:1-7. [CrossRef]

[42] Chen J, Wang ZZ, Kong LL, Chen NH. Hesperidin. In: Du GH, editor. Natural Small Molecule Drugs from Plants. Singapore: Springer; 2018. p. 81–86. [CrossRef]

[43] Hadisi Z, Nourmohammadi J, Nassiri SM. The antibacterial and anti-inflammatory investigation of Lawsonia inermis-gelatin-starch nano-fibrous dressing in burn wound. Int J Biol Macromol 2018;107:2008–2019. [CrossRef]

[44] Albayrak S, Kaya O. Antioxidant and antimicrobial activities of four Astragalus species growing wild in Turkey. Turk J Biochem 2018;43:425–434. [CrossRef]

[45] Adeli-Sardou M, Torkzadeh-Mahani M, Yaghoobi MM, Dodel M. Antibacterial and anti-biofilm investigation of electrospun PCL/gelatin/lawsone nano fiber scaffolds against biofilm producing bacteria. Biomacromol J 2018;4:46–57.